Proceedings Paper:
Wang, J, Yu, H-S orcid.org/0000-0003-3330-1531 and Liu, S (2021) Shakedown Limits of Slab Track Substructures and Their Implications for Design. In: Direct Methods: Methodological Progress and Engineering Applications. PCM-CMM 2019, 08-12 Sep 2019, Kraków, Poland. Springer International Publishing , pp. 211-225. ISBN 9783030488338

https://doi.org/10.1007/978-3-030-48834-5_11

Shakedown limits of slab track substructures and their implications for design

Juan Wang, Hai-Sui Yu, Shu Liu

Abstract This paper presents an approach to shakedown of slab track substructures subjected to train loads. The train load is converted into a distributed moving load on the substructure surface using a simplified track analysis. Based on the lower-bound dynamic shakedown theorem, shakedown solutions for the slab track substructures are obtained over a range of train speeds between zero and the critical speed of the track. It is found the shakedown limit is largely influenced by the ratio of layer elastic moduli and the ratio of train speed to critical speed rather than their absolute values. An attenuation factor, as a function of the critical speed and the friction angle of subsoil, is proposed to effectively obtain the shakedown limit of the slab track substructure at any train speed. In light of the shakedown solutions, improvements to the existing design and analysis approaches are also suggested.

Keywords: slab track; shakedown; design; train loads; trains speed

1 Introduction

Slab tracks have been widely used for high-speed railways. In China, around 70% of the high-speed railways are ballastless slab tracks. Slab tracks require very limited residual settlement/differential settlement as a result of long-term permanent deformation of supporting substructures which comprise compacted granular layers and subsoil.

Nowadays, there is an increasing trend of using shakedown theory in the evaluation of the long-term stability of geotechnical structures under cyclic or variable loads. The shakedown theory has been proven to be very useful for solving design problems in foundations and pavements (e.g. Aboustit and Reddy 1980; Sharp and Booker 1984; Ponter et al. 1985; Collins and Cliffe 1987; Raad et al. 1988; Haldar et al. 1990; Yu and Hossain 1998; Yu 2005; Nguyen et al. 2008; Yu and Wang

J. Wang (✉)
Ningbo Nottingham New Materials Institute, University of Nottingham Ningbo China, 315100, Ningbo, China;
email: juan.wang@nottingham.edu.cn
H. S. Yu
Faculty of Engineering, University of Leeds, LS2 9JT, Leeds, UK;
S. Liu
Ningbo Nottingham New Materials Institute, University of Nottingham Ningbo China, 315100, Ningbo, China; State Key Laboratory for GeoMechanics and Deep Underground Engineering, School of Mechanics and Civil Engineering, China University of Mining and Technology, Xuzhou, Jiangsu, 221116, China.

2012; Wang and Yu 2013a,b; Wang and Yu 2014a,b; Liu et al. 2016). Recently, some shakedown analyses have been performed for the problem of railways subjected to train loads. For example, Zhuang and Wang (2018) obtained the shakedown limits for ballast railways considering the effect of layer thickness and load distribution. Liu et al. (2018a) did shakedown analyses on ballastless slab tracks and assessed the effect of the increasing stiffness modulus with depth. However, the dynamic effect induced by the moving train was not taken into account in the above two articles. Wang et al. (2018) and Liu and Wang (2018) performed dynamic shakedown analyses for the substructure of typical slab tracks based on lower-bound dynamic shakedown theorem. Parametric studies were carried out and the results proved that the ratio of train velocity to the critical velocity of track is a key factor that affects the dynamic shakedown limits. Costa et al. (2018) considered then included the effect of rest stress fields and found that neglecting the rest stress may underestimate the shakedown limit.

In this paper, both quasi-static and dynamic shakedown limits for a typical slab track substructure will be presented. The influencing factors of the shakedown limits and the relation between the dynamic shakedown solution and the quasi-static shakedown solution will be analysed. A fitting equation is then proposed for predicting the dynamic shakedown limits by modifying the quasi-static shakedown limit with an attenuation factor. The implication of this approach for the slab track substructure design will be discussed finally.

2 Simplified model of slab track substructures

Fig. 2.1 shows a typical slab track system which includes a superstructure and a supporting substructure. The superstructure is composed of two rails, a track slab, a concrete base, sleepers, pads and fastening systems. Table 2.1 summarises the properties of the key components of the superstructure. The dimensions of the track slab and the concrete base are taken from a typical Rheda 2000 single track system. The rail is UIC60. The substructure consists of an anti-frozen layer, a prepared subgrade layer and a subsoil layer of infinite depth. Four axle loads belonging to two adjacent bogies on two carriages move at a constant speed V along x-direction (Fig. 2.1). Each axle load is denoted by λP where P is a unit axle load and λ is a scale factor. No traction in the longitudinal or transverse direction is considered. Moreover, the magnitude of the loads is constant, without considering the effect of rail unevenness and vehicle suspension system.

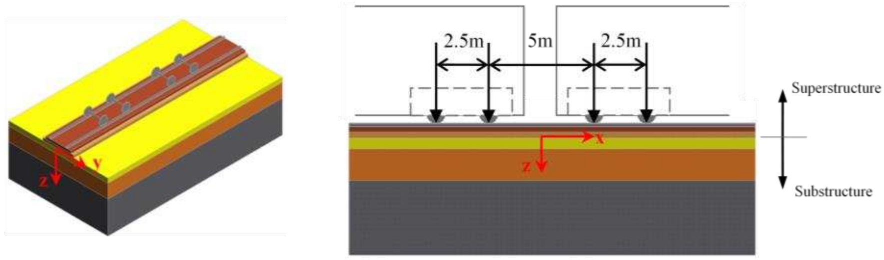

Fig. 2.1 A typical slab track structure and axle loads

Table 2.1 Material properties and dimensions of the key components of slab track superstructure

Layer	Young's modulus E_b (GPa)	Width (cm)	Height (cm)	Second moment of area I (cm^4)	Mass per unit length (kg/m)
Rail	210	15	17.2	3055	60.03
Track slab	34	280	24	322560	1680
Concrete base	10	340	30	765000	2448

This paper focuses on the shakedown analysis of the substructure. A simplified track analysis is proposed to convert the train loads and the superstructure into a distributed moving load on the substructure. It is considered that the superstructure components act together as a single infinite Euler-Bernoulli beam with a total E_bI value (E_b is Young's modulus of the beam materials; I is second moment of inertia of the beam), while the supporting substructure is simplified as a Winkler's foundation. The pads and sleepers are ignored in this study as they do not contribute to the bending of the superstructure. In the assumption of Winkler's foundation, a reaction modulus k is used to describe the resilient response of the soil, which, however, is not a fundamental soil property. Relations between the reaction modulus and the material elastic modulus have been proposed theoretically or empirically by a number of authors for different situations (e.g. Biot 1937; Vesic 1961; Sadrekarimi and Akbarzad 2009). For the problem of an infinite slab track resting on a three-dimensional homogeneous isotropic elastic soil continuum, the relation between the reaction modulus k and the elastic modulus E of the soil has been proposed (Liu et al. 2018):

$$k = \frac{0.583 E_b I}{b^{1.267} d^{3.733}} \tag{2.1}$$

with

$$d = \left(\frac{(1 - \nu^2) E_b I}{E} \right)^{1/3} \tag{2.2}$$

where ν is Poisson’s ratio of the soil; b is the half width of the slab track. For the problem of a layered soil, an equivalent reaction modulus k_{eq} or an equivalent stiffness modulus E_{eq} can be used by equating the maximum deflection of the beam with the maximum surface displacement of the elastic half-space (Liu et al. 2018). In the current study, giving the material properties described in Table 2.1 and the soil Poisson’s ratio of 0.3, Eq. 2.1 can be rewritten as:

$$k = 0.00314\, E^{1.2443} \tag{2.3}$$

Then, the four axle loads can be converted into a distributed load on the top of the substructure according to the following equation:

$$p = p_0 e^{-\mu|x|} (\cos \mu(x) + \sin \mu|x|) \tag{2.4}$$

where $p_0 = \lambda P \mu / 4b$; $\mu = (2kb/E_b I)^{0.25}$.

Fig. 2.2a exhibits the pressure distribution for different values of stiffness modulus. Reaction force due to upward displacement of the beam is taken as zero. As can be seen, the pressure is distributed more widely and uniformly when the reaction modulus is lower. In the transverse direction, the pressure is assumed to be distributed uniformly over the width of the concrete base (i.e. 3.4m), as shown in Fig. 2.2b.

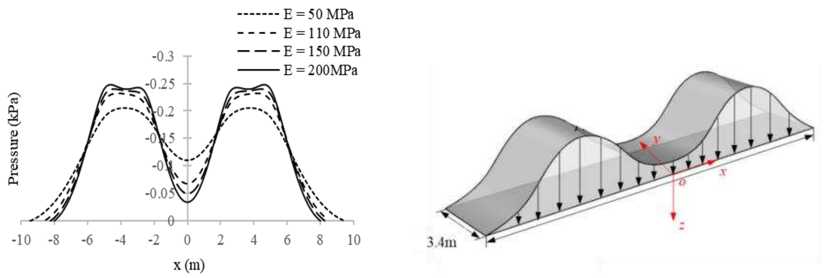

(a) (b)

Fig. 2.2 Pressure distribution on the surface of track substructure

3 Dynamic shakedown analysis

Yu and Wang (2012) proposed an approach to obtain the lower-bound shakedown limits of cohesive-frictional materials under three-dimensional surface loads assuming a quasi-static situation, based on Melan's lower-bound shakedown theorem. However, for the problem of high-speed railways, the dynamic shakedown analysis needs to be performed.

The lower-bound dynamic shakedown theorem of Ceradini (1980) states that shakedown will occur in the real response if a fictitious response and a residual stress field may be found so that

$$f(\lambda\sigma^e_{ij}(t) + \sigma^r_{ij}) \le 0 \tag{3.1}$$

where the residual stress field itself σ^r_{ij} must satisfy self-equilibrium and time-independence conditions; λ is a dimensionless factor; t is time; the fictitious response refers to the elastic response to the external actions (not real elastic-plastic response), such as the unit load-induced elastic stresses $\sigma^e_{ij}(t)$ and displacements $\mathrm{u}^e_i(t)$, should satisfy the following dynamic equilibrium conditions:

$$\sigma^e_{ij,j}(t) + X_i(t) = \rho \ddot{u}_i(t) - \chi \dot{u}_i(t) \tag{3.2}$$

$$\sigma^e_{ij}(t) - f_i(t) = 0 \tag{3.3}$$

where is X_i body force field applied to the region V with an initial state; ρ is material density; χ is damping coefficient and f_i is surface force acting on the surface S. Tension positive notation is applied throughout this paper.

For the problem considered here, assuming the soil behaviour obeys the Mohr-Coulomb yield criterion, the lower-bound dynamic shakedown theorem requires that the total stress state of any point must not lie outside the Mohr-Coulomb yield surface at any time. On each x-z plane, since σ^r_{yy} can be chosen such that σ_{yy} is always an intermediate principle stress, the substitution of the total stresses into the Mohr-Coulomb yield criterion leads to the following expression:

$$f = (\mathrm{\sigma}^{\mathrm{r}}_{\mathrm{xx}} + \mathrm{M})^2 + \mathrm{N} \le 0, \tag{3.4}$$

with

$$\mathrm{M} = \lambda\mathrm{\sigma}^{\mathrm{e}}_{\mathrm{xx}} - \lambda\mathrm{\sigma}^{\mathrm{e}}_{\mathrm{zz}} + 2\tan\phi(\mathrm{c} - \lambda\mathrm{\sigma}^{\mathrm{e}}_{\mathrm{zz}}\tan\phi), \tag{3.5}$$

$$\mathrm{N} = 4(1 + \tan^2\phi)[(\lambda\mathrm{\sigma}^{\mathrm{e}}_{\mathrm{xz}})^2 - (\mathrm{c} - \lambda\mathrm{\sigma}^{\mathrm{e}}_{\mathrm{zz}}\tan\phi)^2], \tag{3.6}$$

where ϕ and c are soil dynamic friction angle and cohesion, respectively; σ_{ij}^{e} is elastic stress field induced by the unit axle loads P, moving at a constant speed V. The elastic stress field can be obtained by using analytical solutions of Easton (1965) for the case of a homogenous isotropic half-space or performing finite element simulations for a layered structure. A typical finite element model of the track substructure is shown in Fig. 3.1. The details of the model can be found in Wang et al. (2018).

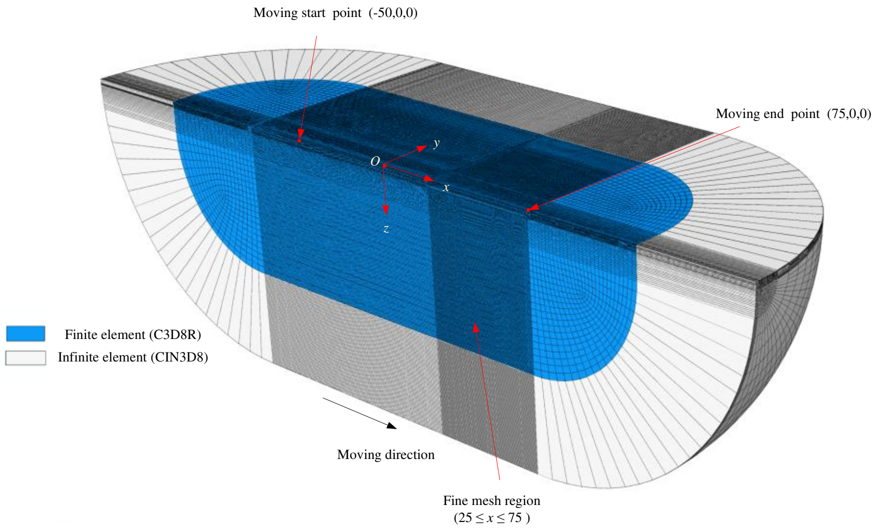

Fig. 3.1 Finite element model of track substructure

The residual stress σ_{xx}^{r} must be time-independent and self-equilibrated. For problems where the travelling speed of the surface load is constant and smaller than the wave propagation velocity, every points at the same depth experience an identical stress history. The elastic stress field over a period T at any given speed does not change with position. Using the Mohr-Coulomb yield criterion and the self-equilibrium condition of the residual stress field, it is found that the actual horizontal residual stress must be fully bracketed by the two critical residual stress fields, when the structure is at a shakedown status (Wang et al. 2018).

$$\sigma_{\mathrm{xx}-l}^{r} = \max_{z=j}^{-\infty\leq x\leq\infty}(-M_i - \sqrt{-N_i}) \tag{3.7}$$

$$\sigma_{\mathrm{xx}-\mathrm{u}}^{r} = \max_{z=j}^{-\infty\leq x\leq\infty}(-M_i + \sqrt{-N_i}) \tag{3.8}$$

in which i represents a general point at depth $z = j$. By substituting the load-induced elastic stress fields and either of the critical residual stress fields into the Mohr-Coulomb yield criterion $f(\sigma) \leq 0$, the present shakedown problem can be rewritten as a mathematical optimisation problem:

$$\max \lambda \\ s.t. \begin{cases} f(\sigma^r_{xx}(\lambda\sigma^e), \lambda\sigma^e) \leq 0 \text{ for all points} \\ \sigma^r_{xx}(\lambda\sigma^e) = \sigma^r_{xx\text{-}l} \text{ or } \sigma^r_{xx\text{-}u} \end{cases} \tag{3.9}$$

If λ is larger than the shakedown limit, f will be larger than 0 at some points; otherwise, f will always be equal or smaller than 0. The maximum admissible load factor is the shakedown limit multiplier of the substructure, denoted by λ_{sd}. The above shakedown condition can be reduced to a quasi-static shakedown solution when the train speed is very low. At any given speed, the above mathematical formulation then can be solved by using a procedure in Yu and Wang (2012) and will not be repeated here.

For a layered structure, it is useful to know which layer is critical. The shakedown limit multiplier λ_{sd}^{n} of each layer can be calculated and compared. Finally, the shakedown limit of the whole structure is the lowest one among them:

$$\lambda_{\text{sd}} = \min(\lambda^1_{sd}, \lambda^2_{sd}, \ldots, \lambda^n_{sd}) \tag{3.10}$$

where the subscript n (= 1, 2, 3…) means the n^{th} layer.

4 Shakedown limits

A typical slab track substructure, composed of an anti-frozen layer, a prepared subgrade, and a subsoil of a great depth, is considered in this study. According to Eq. 3.4-3.6, the shakedown limit of a slab track is dependent on the plastic properties of the soils (i.e. ϕ and c) and the elastic stress distributions in the soils. The latter is controlled by the pressure distribution, the elastic parameters of the soils, and the moving speed of the train loads V with respect to the critical speed of the substructure V_{cr}. It should be noted that the stiffness modulus of a soil also depends on the frequency of loading. Therefore, in the stability analysis of high-speed railways, a dynamic stiffness modulus E_d, which is higher than the stiffness modules E, is normally employed instead. In light of this, the current research will investigate the quasi-static situation and the dynamic situation, respectively; and the effect of the stiffness modulus will be discussed. Table 4.1 shows the material properties and layer thicknesses of the three-layered substructure in this study.

Table 4.1 Material properties and layer thicknesses of a three-layered sub-structure

Layer name	h_n (m)	E_n (MPa)	$E^d{}_n$ (MPa)	v_n	ϕ_n (°)	c_n (kPa)	ρ_n (kg/m^3)
Anti-frozen layer	0.4	200	290	0.3	50	1	2000
Prepared Subgrade	1.3, 1.8, 2.3, 2.8	130	190	0.3	40	2	1850
Subsoil	∞	110 or 55	160	0.3	30	2	1800

4.1 Shakedown limits in a quasi-static situation

For the case of a stiff subsoil (i.e. E_3 = 110MPa), the influence of the thickness of the prepared subgrade is first investigated. Fig. 4.1 demonstrates that the increase of the subgrade thickness (2nd layer) decreases the shakedown limit of that layer but increases those of the other two layers. More significant changes occur in the subsoil (3rd layer). According to Eq.3.10, the lowest shakedown limit among all layers is the overall shakedown limit of the substructure. Therefore, there exists an optimum subgrade thickness in this case, at around 1.7m, above which further increase of the thickness barely changes the overall shakedown limit.

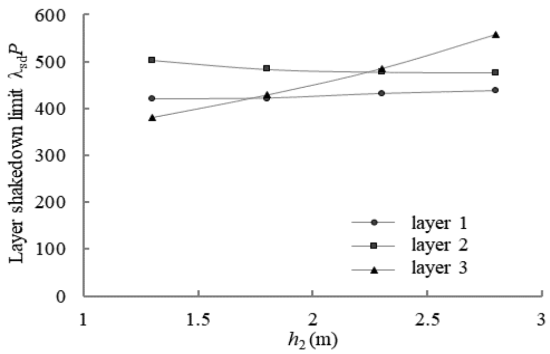

Fig. 4.1 Effect of subgrade thickness on the shakedown limit of each layer when E_1 = 200MPa, E_2 = 130 MPa, E_3 = 110MPa

Fig. 4.2 further examines the influence of the values of the stiffness moduli on the shakedown limit by using the values of the dynamic stiffness moduli E^d instead. The corresponding load distributions are applied. It should be noted that the ratio of the dynamic stiffness moduli E_1^d / E_2^d / E_3^d is set to be identical to

$E_1/E_2/E_3$. Compared to Fig. 4.1, this case shows similar trends of the shakedown limits of each layer; while the optimum layer thickness is moved to around 2.2m. In Fig. 4.3, a direct comparison of the overall shakedown limits shows that increasing the stiffness moduli by 40% reduces the shakedown limit (by 7% at maximum) for the cases of a low h_2, but increases it (by 4% at maximum) for the cases of a high h_2. Further investigation reveals that the small differences are only attributed to the changed pressure distribution, not the values of the stiffness modulus, because the elastic stress fields under a specific distribution is only dependent on the ratio of layer stiffness moduli. For the cases of a high stiffness modulus, the pressure is less evenly distributed, leading to a lower shakedown limit of the first layer and higher shakedown limits of the other two layers. The above finding implies that, though the stiffness moduli of soils vary with the frequency of loading or the train speed, if the rates of the changes are similar for soils in different layers, it will barely have influence on the shakedown limit. Additionally, when the thickness of the prepared subgrade is relatively large, the subsoil layer becomes less critical, resulting in an increase of the shakedown limit of the subsoil; otherwise, the other two layers are more likely to fail.

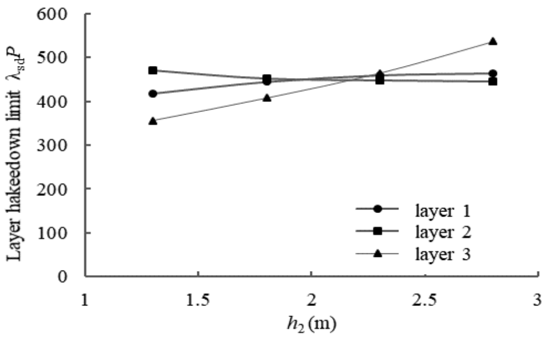

Fig. 4.2 Effect of subgrade thickness on the shakedown limit of each layer when E_1^d = 290MPa, E_2^d = 190 MPa, E_3^d = 160MPa

Fig. 4.3 also shows the shakedown limit of the substructure when the subsoil is soft (i.e. E_3 = 55MPa). Compared to the case of a stiff subsoil, the shakedown limit is dropped significantly. If the design axle load is 250 kN, the substructure will definitely fail due to excessive permanent deformation. The shakedown limits of the three layers are 220 kN, 290 kN and 572 kN, respectively. This implies that for the case of a poor subsoil, more stresses are locked in the upper layers thus a higher possibility of failure in the subgrade.

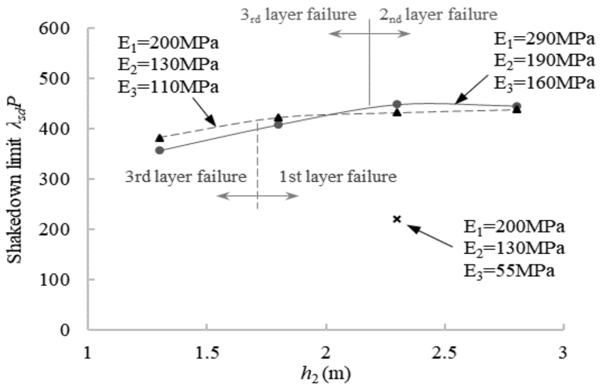

Fig. 4.3 Effects of stiffness modulus and subgrade thickness on the shakedown limit

4.2 Shakedown limits in a dynamic situation

When the dynamic situation is considered, the elastic stress fields, and thus the shakedown limit, highly depend on V/V_{cr}, where V represents the moving speed of the train loads V and V_{cr} represents the critical speed of the track. Fig. 4.4a demonstrates an accelerated decrease of the shakedown limit of each layer with rising train speed, when the dynamic stiffness moduli in Table 4.1 are utilised. The shakedown limit is minimum when the train speed is close to the shear wave velocity of the bottom layer $V_{\text{s-layer3}}$, which can be recognised as the critical velocity of the slab track. If the stiffness moduli are reduced by the same rate (say 44%) while maintaining the pressure distribution, the shakedown limits of the three layers will be decreased, as shown in Fig. 4.4a. If the shakedown limits are replotted against a velocity factor α, defined as V/V_{cr}, the two cases will coincide with each other (Fig. 4.4b). As a result, the shakedown limit is controlled by the velocity factor rather than the values of the train speed.

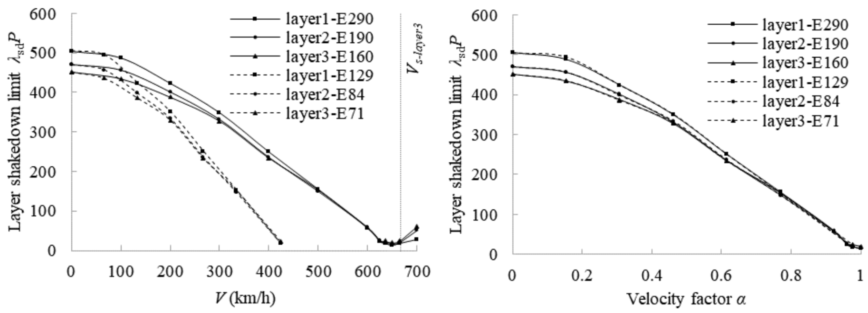

(a) (b)

Fig. 4.4 Effect of train speed on dynamic shakedown limit when h_2=2.3m

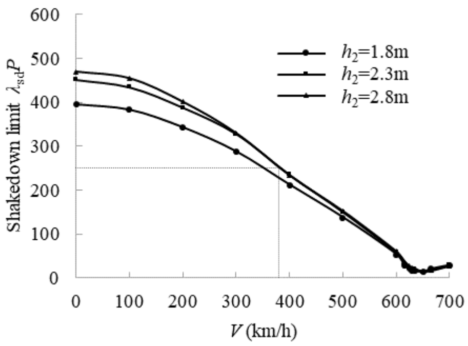

Fig. 4.5 Effect of subgrade thickness on dynamic shakedown limit

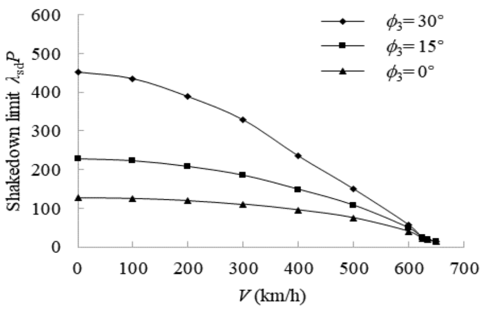

Fig. 4.6 Effect of friction angle on dynamic shakedown limit when h_2=2.3m

Indeed, a thicker prepared subgrade benefits to the long-term stability of the substructure. Despite of that, as the train speed is raised, this benefit becomes very limited, as shown in Fig. 4.5. For the case studied here, the slab track is able to sustain axle loads of 250 kN when the train speed is smaller than 280 km/h. If more loads or a higher train speed are to be applied, increasing the subgrade thickness alone will not help with the situation, because it cannot prevent the accumulating permanent deformation in the second layer. Instead, the material quality of this layer should be improved. More detailed comparisons for the shakedown limits of each layer considering different train speeds can be found in Wang et al. (2018).

Fig. 4.6 demonstrates that a decrease of the friction angle of the subsoil leads to a drop of the shakedown limit of the substructure. However, it does not affect the critical speed of the substructure. Therefore, the shakedown limit decreases more significantly with an increasing train speed for the case of a larger friction angle. This implies that though the high friction angle has a positive effect on the long-term stability of the track substructure, one should be very careful when trying to increase the train speed at those cases.

4.3 Relationship between static and dynamic shakedown limits

The effect of the train speed on the shakedown limit can be quantified by introducing an attenuation factor η, defined as the dynamic shakedown limit for the current speed $\lambda_{sd}^{d}P$ over that of the quasi-static case $\lambda_{sd}^{s}P$, so that the dynamic shakedown limit at any given speed can be estimated according to:

$$\lambda_{sd}^{d}P = \eta\lambda_{sd}^{s}P \tag{4.1}$$

Fig. 4.7a shows the variation of the attenuation factor against the velocity factor for different values of subsoil friction angle. When the velocity factor is smaller than 0.1, the attenuation factor is close to 1; otherwise, it decreases with the rising velocity factor. Similar trends can be obtained in other cases (Fig. 4.8). And thus, a fitting equation is proposed as below:

$$\eta = \begin{cases} 1 \text{ when } \alpha \le 0.1 \\ (1-\eta_{cr}) \times \sqrt[n]{1-(\dfrac{\alpha-0.1}{0.9})^{n}} + \eta_{cr} \text{ when } 0.1 < \alpha < 1 \end{cases} \tag{4.2}$$

where n is a coefficient depending on the friction angle of the subsoil, the value of which can be obtained from Fig. 4.7b; η_{cr} is the attenuation factor when $V = V_{cr}$, the value of which can be taken as 0 in common design situations (exception occurs when the stiffness of subsoil is extremely low compared to the stiffness of the upper layers). Fig. 4.8 also reveals the attenuation factor was barely affected by the thickness of the prepared subgrade.

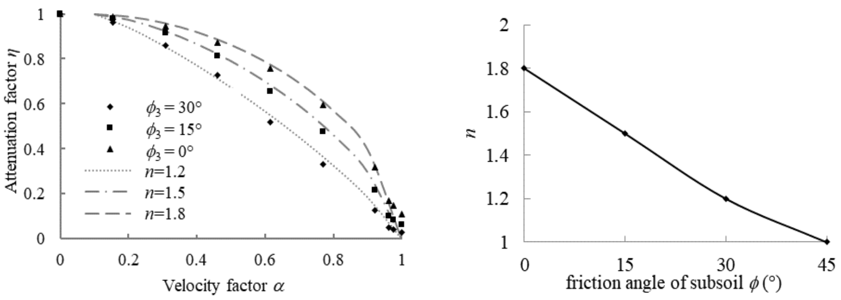

(a) (b)

Fig. 4.7 Variation of attenuation factor when h_2=2.3m

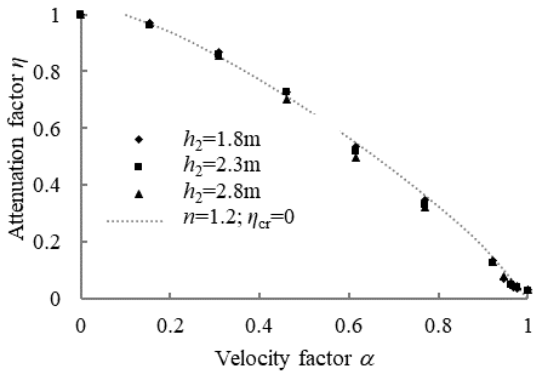

Fig. 4.8 Effect of subgrade thickness on attenuation factor

5 Implications for design

5.1 Safe train speed

In practice, a quick evaluation of the maximum admissible train speed is useful for the design of high-speed railways. One rule-of-thumb approach is to use the 70% of the critical speed of the track (Heelies et al. 1999; Mezher et al. 2016). However, in the shakedown analysis of a typical slab track substructure, Fig. 4.5 demonstrates that a safe train speed should be smaller than 60% of the critical speed, considering axle loads of 250 kN. Therefore, the use of 70% of the critical speed cannot guarantee the long-term stability of the slab track.

5.2 Amplification factor

In the long-term stability analysis of slab track substructures, it is commonly required to determine the dynamic stresses on soils. For a slab track of good condition, the dynamic effect from rail unevenness or vehicle suspensions system is minor, and therefore the dynamic stresses on soils can be obtained by applying an amplified load P^d, which is the product of the static axle load P^s and an amplification factor β :

$$P^{\mathrm{d}} = \beta P^{s} \tag{5.1}$$

where β is a function of train speed. A range of values for the amplification factor can be found in literature, as shown in Fig. 5.1.

It should be noted that the reciprocal of the attenuation factor can be related with the amplification factor, since $P^d \le \lambda_{sd}^d P$ and $P^s \le \lambda_{sd}^s P$. If the applied load is the shakedown limit of the slab track substructure (i.e. $P^d = \lambda_{sd}^d P$ and $P^s = \lambda_{sd}^s P$), then

$$\beta = \frac{P^d}{P^s} = \frac{\lambda_{sd}^d P}{\lambda_{sd}^s P} = \frac{1}{\eta} \tag{5.2}$$

In light of this, $1/\eta$ from the shakedown analysis of the typical slab track substructure is compared with β in literature. A range of subsoil friction angle between 0° and 45° is considered. As can be seen, when the friction angle is 45°, the values of $1/\eta$ are close to the amplification factors of German design code (Gobel et al. 1996). The amplification factors of Hu and Li (2010) are close to the values of $1/\eta$ for the cases of a relatively low friction angle. These results imply that the evaluation of the dynamic effect on the long-term stability of a slab track should have also considered the friction angle of subsoil.

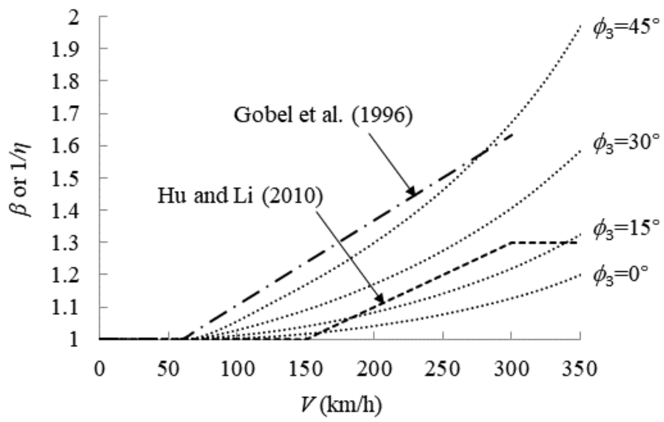

Fig. 5.1 Comparison with literatures

6 Conclusions

Shakedown solutions of typical slab track substructures under moving train loads are presented in this paper. Key findings are summarised below:

1. A quasi-static shakedown condition can be assumed if the moving train velocity is no larger than 10% of the critical speed of the track.

2. Using the dynamic stiffness moduli of soils instead of the stiffness moduli will barely affect the shakedown limit of the substructure, as long as the ratio of layer stiffness maintains.
3. The dynamic shakedown limit at any given train speed can be obtained by multiplying the shakedown limit in the quasi-static situation by an attenuation factor. For typical slab track substructures, the attenuation factor is only dependent on the friction angle of subsoil and velocity factor.
4. A train speed of 70% of the critical speed cannot guarantee the long-term stability of slab tracks.
5. At a given train speed, the amplification factors of the axle load due to the dynamic effect of the train speed can be distinct from each other for the cases of different subsoil friction angle.

Acknowledgement

Financial support from National Natural Science Foundation of China (Grant No. 51408326) and Ningbo Natural Science Foundation (Grant No. 2018A61035) is gratefully acknowledged.

Reference

1. Aboustit BL, Reddy DV (1980) Finite element linear programming approach to foundation shakedown. in: Proceedings of the International Symposium on Soils under cyclic and transient loading. Swansea, 2: pp727-738
2. Biot M (1937) Bending of an infifinite beam on an elastic foundation. J Appl Mech Trans Am Soc Mech Eng 59: cA1–7
3. Collins IF and Cliffe PF (1987) Shakedown in frictional materials under moving surface loads. Int J Numer Anal Methods Geomech 11(4):409-420
4. Costa PA, Lopes P, Cardoso AS (2018). Soil shakedown analysis of slab railway tracks: Numerical approach and parametric study. Transp Geotech 16, 85-96
5. Göbel EF (1974) Rubber springs design. John Wiley and Sons, London
6. Haldar AK, Reddy DV, Arockiasamy M (1990) Foundation shakedown of offshore platforms. Compu Geotech 10(3): 231-245
7. Hu YF, Li NF (2010) Subgrade design principle of the high-speed railway of unballasted track (Chinese). China: Railway Publishing House, Beijing
8. Heelis ME, Collop AC, Dawson AR et al (1999) Predicting and measuring vertical track displacements on soft subgrades, in: Railway Engineering 99 May. London
9. Liu S, Wang J, Yu HS, Wanatowski D (2018) Shakedown for slab track substructures with stiffness variation. Geotech Res 5(1): 31-38
10. Liu S, Wang J (2018) Application of shakedown theory in track substructure design." Proceedings of the Institution of Civil Engineers-Ground Improvement 172.2 (2019): 116-123.
11. Shakedown for slab track substructures with stiffness variation. Geotech Res 5(1): 31-38
12. Liu S, Wang J, Yu HS, Wanatowski D (2016) Shakedown solutions for pavements with materials following associated and non-associated plastic flow rules. Comput Geotech 78:218-266

13. Melan E (1938) Der spannungsgudstand eines Henky-Mises Schen Kontinuums Bei Verlandicher Belastung. Sitzungberichte der Ak Wissenschaften Wie 47(73)
14. Mezher SB, Connolly DP, Woodward PK et al (2016) Railway critical velocity - analytical prediction and analysis. Transp Geotech 6:84–96
15. Nguyen AD, Hachemi A,Weichert D (2008) Application of the interior-point method to shakedown analysis of pavements. Int J Numer Methods Eng 75:414–439
16. Ponter ARS, Hearle AD, Johnson KL (1985) Application of the kinematical shakedown theorem to rolling and sliding point contacts. J Mech Phys Solids 33:339–362
17. Raad L, Weichert D, Najm W (1988) Stability of multilayer systems under repeated loads.
18. Transp Res Rec 1207:181–186
19. Sadrekarimi J, Akbarzad M (2009) Comparative study of methods of determination of coeffiffifficient of subgrade reaction. Electron J Geotech Eng 14(s1–6):211–6
20. Vesic AB (1961) Bending of beams resting on isotropic elastic solid. J Eng Mech 87(2):35–54
21. Wang K, Zhuang Y, Liu H (2018) Shakedown analysis for the evaluation of strength and bearing capacity of multilayered railway structures. Proc. Inst. Mech. Eng., Part F 232(9): 2324-2335
22. Wang J, Liu S, Yang W (2018) Dynamics shakedown analysis of slab track substructures with reference to critical speed. Soil Dyn Earthq Eng 106: 1-13
23. Wang J, Yu HS (2014) Three-dimensional shakedown solutions for anisotropic cohesivefrictional materials under moving surface loads. Int J Numer Anal Methods Geomech 38:331–348
24. Wang J, Yu HS (2013a) Shakedown analysis for design of flexible pavements under movingloads. Road Mater Pavement Des 14:703–722
25. Wang J, Yu HS (2013b) Shakedown and residual stresses in cohesive-frictional half-space under moving surface loads. Geomech Geoeng: Int J 8:1–14
26. Yu HS (2005) Three-dimensional analytical solutions for shakedown of cohesive-frictional materials under moving surface loads. Proc R Soc A: Math, Phys Eng Sci 461:1951–1964
27. Yu HS, Hossain MZ (1998) Lower bound shakedown analysis of layered pavements using discontinuous stress fields. Comput Methods Appl Mech Eng 167:209–222
28. Yu HS, Wang J (2012) Three-dimensional shakedown solutions for cohesive-frictional materials under moving surface loads. Int J Solids Struct 49:3797–3807
29. Zhuang Y, Wang KY (2017) Three-dimensional shakedown analysis of ballasted railway structures under moving surface loads with different load distributions. Soil Dyn Earthq Eng100: 296-300